

# Highly Stretchable, Ultratough, and Multifunctional Poly(vinyl chloride)-Based Plastics *via* a Green, Star-Shaped Macromolecular Additive

Wei-Guang Chen, Hai-Jie Wei, Jiancheng Luo, Yu Chen,\* and Peng-Fei Cao\*



Cite This: *Macromolecules* 2021, 54, 3169–3180



Read Online

ACCESS |



Metrics & More

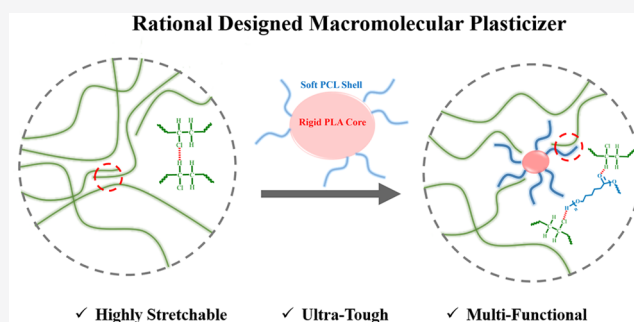


Article Recommendations



Supporting Information

**ABSTRACT:** As one of the most prolifically produced plastics in the world, poly(vinyl chloride) (PVC) suffers from mechanical brittleness and low toughness. Compared with traditional phthalate-type plasticizers, poly( $\epsilon$ -caprolactone) (PCL)-based plasticizers are especially attractive due to their “green” nature and capabilities to achieve improved physical properties. Herein, a stretchable and ultratough PVC-based plastic was achieved by a star-shaped PCL copolymer with a rigid, amino-containing, branched polylactide (N-BPLA) core and a soft PCL shell, that is, RN-SPCLs. With an optimal feed ratio of the CL monomer and N-BPLA core, the RN-SPCL2 can efficiently lower the glass transition temperature ( $T_g$ ) of PVC plastics, achieving the transition from the “glassy” to “rubbery” state at ambient temperature. The obtained RN-SPCL2/PVC not only shows high extensibility, that is, 453%, but also maintains close to 80% of tensile strength of neat PVC, that is, 30.1 MPa, which is much higher than the previously reported plasticized PVCs. Its overall toughness reaches 92.7 MJ/m<sup>3</sup>, being more than 50-fold higher than neat PVC and 2 to 3 times higher than linear PCL or dibutyl phthalate plasticized PVCs. The important role of star-shaped architecture with a rigid core and flexible PCL shell for RN-SPCL2 in achieving highly stretchable and ultratough PVC plastics is systematically investigated. More interestingly, the as-prepared RN-SPCLs also endow PVC plastics with photoluminescence property and allow homogeneous dispersion of nanosized TiO<sub>2</sub> for significantly enhancing the anti-UV capability.



## INTRODUCTION

Developing elastomers with improved mechanical performance, low cost, high stability, and preferred functionalities is highly demanded for current industrial applications such as in sealants, medical devices, automobiles, and other emerging areas including flexible strain sensors, stretchable batteries, roll-up displays and communication devices.<sup>1–8</sup> Currently, most of the elastomers are derived from polymers with low glass transition temperature ( $T_g$ ) far below the ambient temperature, such as poly(isoprene),<sup>9</sup> and poly(butyl acrylate),<sup>10</sup> poly(dimethylsiloxane),<sup>11</sup> and poly(butadiene).<sup>12</sup> With liquid-like behavior and weak mechanical performance for these intrinsic elastic polymers, chemical/physical cross-linking or copolymerization with another type of glassy polymer ( $T_g >$  ambient temperature) is usually applied to achieve elastomers with improved modulus and high toughness.<sup>11–15</sup> Mays and co-workers have reviewed different types of living polymerization techniques, including anionic polymerization, that have been utilized for the synthesis of hard blocks and soft blocks containing copolymeric elastomers with different architectures, such as triblock linear polymers, star copolymers, and bottlebrush copolymers.<sup>16</sup> However, with a relatively complicated process, most of the fabricated elastomers still suffer

from chemical instability and unsatisfied mechanical performance. As an alternative approach, lowering the  $T_g$  of traditional glassy polymers with excellent physical properties has been less investigated, although it will bring further opportunities to achieve cost-efficient, high-performance elastomers.<sup>15,17–19</sup>

With excellent heat and chemical resistance, good electrical insulation properties, decent mechanical performance, and low cost, poly(vinyl chloride) (PVC) is one of the most widely used synthetic plastic polymers in the world, only second to polyolefins in volume.<sup>20,21</sup> PVC has been utilized in different fields such as cable and wire insulation, window frames, pipes, flooring, packaging, bottles, and credit cards.<sup>22</sup> One of the main drawbacks of pure PVCs is their mechanical brittleness under the service condition and high melting viscosity under the processing condition, ascribed to its “glassy” nature at ambient temperature ( $T_g >$  70 °C). As one of the most

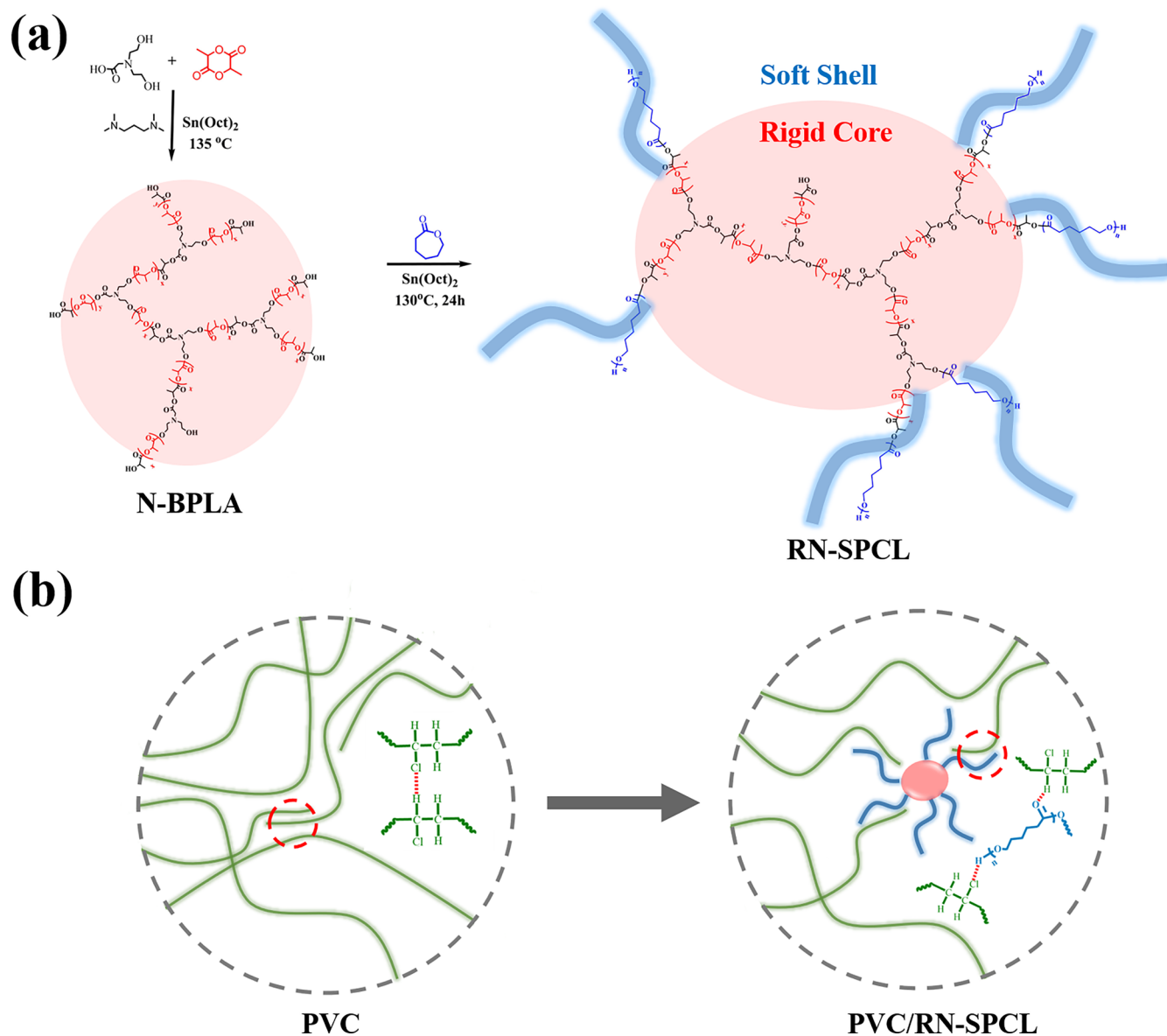
**Received:** January 5, 2021

**Revised:** March 9, 2021

**Published:** April 2, 2021



Scheme 1. (a) Synthesis of RN-SPCL Using N-BPLA as the Macroinitiator; (b) Schematic Representation of the Plasticization Mechanism by RN-SPCL



prolifically produced plastics in the world, transforming the “glassy” PVC into cost-efficient and high-performance elastomers will definitely broaden their application fields, especially in the areas requiring flexibility and stretchability such as sealants, flexible electronics/sensors, and medical devices.<sup>17,23,24</sup> Different from other glassy polymers, such as polystyrene, whose glassy nature is derived from the rigid backbone, the strong polar interaction between polymer chains leads to the high  $T_g$  of PVC.<sup>25</sup> Therefore, developing the plasticizers that can efficiently suppress the physical interaction should allow reduced  $T_g$  and achieve PVC-based elastomers or plasticized PVCs.<sup>26,27</sup> With more than 500 types of plasticizers being industrialized, phthalates including di(2-ethylhexyl)-phthalate, dibutyl phthalate (DBP), and di-*n*-octyl phthalate cover more than 80% of the plasticizer market for PVCs due to their excellent plasticizing effect and relatively low cost.<sup>26,27</sup> However, the phthalate plasticizers can gradually migrate from the PVC matrix over time, which will not only render

unfavorable effect for the environment but also diminish the mechanical performance of PVCs.<sup>28,29</sup>

Among the numerous phthalate-free, environment-friendly plasticizers being developed, the macromolecular plasticizers<sup>30–34</sup> are superior compared to small-molecular analogues<sup>27,35–49</sup> because of the low molecular mobility of polymers. Meanwhile, multisite concerted interactions between PVC and plasticizers can overcome the leaching issue and maintain long-term mechanical performance.<sup>50,51</sup> With excellent biodegradability, high miscibility with PVC, good chain flexibility, and potential synthesis from a biosource, poly( $\epsilon$ -caprolactone) (PCL)-based polymers are especially attractive as “green” plasticizers for PVC.<sup>33,52–54</sup> In the polymer field, rational structure design of polymeric materials with different topologies is always critical toward their optimal properties and enhanced performance following the “structure–property” relationship.<sup>16,55,56</sup> In this aspect, the PCL plasticizers with branched structures can increase the mobility of PVC systems in a more efficient manner than the linear ones due to their

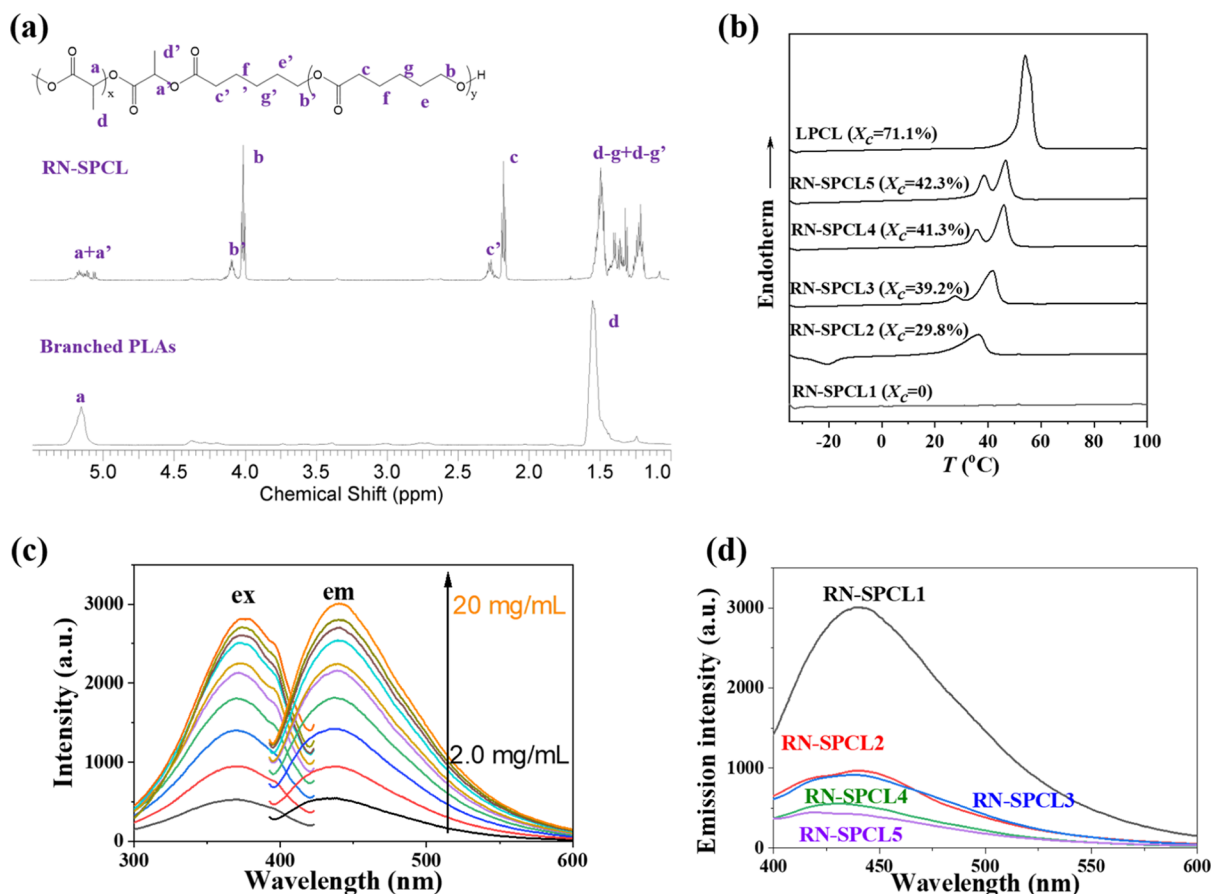


**Figure 1.** (a) Typical <sup>1</sup>H NMR spectra of purified RN-SPCL and N-BPLA; (b) second-heating DSC thermograms of RN-SPCLs and LPCL; (c) fluorescent spectra of RN-SPCL1; (d) fluorescence emission spectra of RN-SPCLs at 20 mg/mL in CH<sub>2</sub>Cl<sub>2</sub>.

large number of chain end, high free volume, and increased mobility.<sup>17,23,57,58</sup> For instance, the highly branched copolymer obtained from one-pot copolymerization of CL and glycidol affords the PVC blends (60 wt % plasticizer relative to PVC) with high extensibility (~310 to 390%) and decent tensile strength (~12 to 16 MPa).<sup>23</sup> The multiarm star-shaped PCLs (SPCLs) synthesized from the dipentaerythritol or hyperbranched polyester are also reported to significantly improve the extensibility of PVC systems (up to 380%).<sup>17,59</sup> With numerous reports on achieving highly stretchable PVC elastomers *via* the PCL plasticizers, their improved extensibility (~350%) is always obtained at the price of significantly reduced tensile strength (usually ≤ 50% of original tensile strength). Achieving a PCL plasticizer that affords PVC systems with improved extensibility, less sacrifice of tensile strength, and meanwhile, high toughness *via* rational architecture design is still a scientific challenge.

Herein, rationally designed SPCLs with relatively rigid core and flexible PCL arms were synthesized by ring-opening polymerization of CL from a sustainable, biodegradable polylactide/*N,N*-bis(2-hydroxyethyl)glycine (PLA/BHEG)-based branched polymer. As a “green” plasticizer, the SPCL allows significantly increased elongation before breaks (>450%, more efficient than the previously reported PCLs with different topologies) while retaining their high tensile strength (~80% of original tensile strength), achieving PVC-based elastomers with an overall toughness up to 92.7 MJ/m<sup>3</sup>, more than 50-fold higher than neat PVC and 2 to 3 times higher than linear PCL (LPCL) or DBP-plasticized PVCs. More interestingly, with a

unique core–shell structure, amino-containing rigid core, and efficient interaction with TiO<sub>2</sub> nanoparticles, the as-prepared SPCLs also endow the PVC-based elastomers with photoluminescence property and capability of homogeneous dispersion of TiO<sub>2</sub> for enhanced UV tolerance. It is anticipated that the design principle developed in current research not only affords a mechanically robust, multifunctional PVC-based stretchable material but also sheds light on rational design of polymer topologies toward high-performance, sustainable plasticizers.

## RESULTS AND DISCUSSION

**Synthesis and Characterization of SPCLs.** PCL is a well-known biodegradable soft polymer with low melting and glass transition temperatures ( $T_m$  and  $T_g$ ), and it is highly miscible with a variety of commercial polymers.<sup>54,60,61</sup> Although the present commercially available CL monomer is a petroleum-based product due to the cost factor, in fact, it can be prepared from sustainable resources.<sup>62</sup> Targeted by the preparation of multifunctional green plasticizer for PVC plastics, we designed a SPCL possessing a relatively rigid core, that is, a sustainable branched polymer derived from PLA with BHEG as branching units.<sup>63</sup> It is worth noticing that the tertiary amine groups endow the branched PLAs intrinsic photoluminescence nature and guest-encapsulation capacity, which will be further discussed later. The N-containing branched PLAs (N-BPLAs) with a branching degree of 9% ( $M_n = 7.8 \times 10^3$ ,  $D = 1.4$ ) were employed as macroinitiators for the ring-opening polymerization of CL, achieving SPCLs

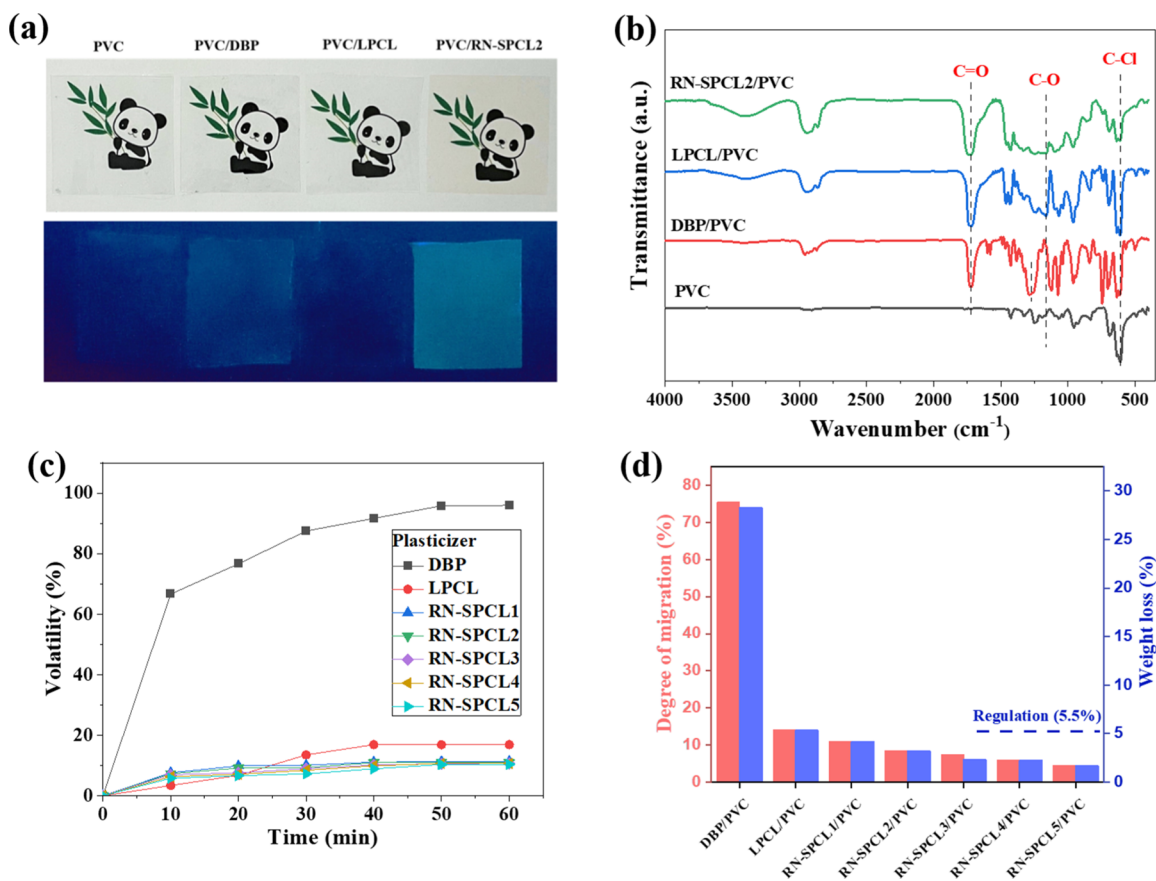


**Figure 2.** (a) Pictures of prepared films under sunlight and UV light; (b) FT-IR spectra of PVC and plasticized PVCs; (c) volatility of plasticizers in plasticized PVC at 200 °C over 60 min; (d) degree of migration and weight loss of plasticized PVCs heated in *n*-hexane at 50 °C for 2 h (the weight ratio of the plasticizer to PVC is 0.6:1).

with a relatively rigid, nitrogen-containing core that is abbreviated as RN-SPCL (Scheme 1a).

From the  $^1\text{H}$  NMR of unpurified polymers after the bulk polymerization (Figure S1), the complete disappearance of the proton signals from CL monomer implies monomer conversion close to 100% under the adopted polymerization conditions. As illustrated by the  $^1\text{H}$  NMR spectra of purified RN-SPCLs (Figures 1a and S2), the typical signals from the branched PLA core and PCL arms can be observed clearly, whereas the signals from the hydroxyl-connected units in the branched PLA core (at 4.38 and 3.74 ppm, Figure S3) disappear, implying that almost all of terminated OH of N-BPLA initiated the ring-opening polymerization of the CL monomer. The successful initiation is also confirmed by the appearance of proton signals at the junction of LA and CL units ( $a'$ ,  $b'$ , and  $c'$  in Figure 1a), whose intensities decrease significantly with the increased PCL contents (Figure S2). From the comparative integrals of the methine proton signals in LA units (around 5.1 ppm) and the carbonyl-adjacent methylene proton signals in CL units (around 2.2 ppm), the monomer ratios of CL to LA in copolymers are calculated. Through gradually raising the feed ratio of CLs to branched PLAs, the RN-SPCL copolymers with different PCL contents were obtained and named as RN-SPCL1, RN-SPCL2, RN-SPCL3, RN-SPCL4, and RN-SPCL5, respectively (Table S1). It can be seen that the actual ratios of CL to LA in copolymers are higher than their feed ratios, which can be ascribed to the low segmental mobility of BPLA in the core, leading to the underestimated LA content in the  $^1\text{H}$  NMR spectrum.<sup>64</sup> The

GPC curves of the obtained RN-SPCLs show presented unimodal peaks for all the polymers (Figure S4). Raising the feed ratio of CL to N-BPLA results in an increased molecular weight and relatively decreased polydispersity ( $\bar{D}$ ) at the same time (Table S1).

Differential scanning calorimetry (DSC) was used to investigate the effect of branched architecture on the crystallization behavior of RN-SPCLs (Figures 1b and S5). It is clear that the LPCL and RN-SPCLs with relatively high contents of PCL are semicrystalline polymers. In the second heating thermograms, LPCL shows a sharp and intense melting peak at 54.1 °C, with the degree of crystallinity ( $X_c$ ) being 71.1%. As for the RN-SPCLs, the introduction of a branching structure remarkably reduces the melting temperature and  $X_c$ . The melting point and  $X_c$  of RN-SPCLs are further reduced with lower PCL contents. With respect to RN-SPCL1 which has the lowest PCL content, no melting peak can be observed, indicating its amorphous nature. In addition, polarized optical microscopy (POM) also confirms the crystallization behavior of different samples at 25 °C (Figure S6), where LPCL and RN-SPCLs with higher contents of PCL show better crystallinity.

The photoluminescence properties of the prepared amino-containing RN-SPCLs were also investigated since the amino-rich polymers have been reported to exhibit intrinsic photoluminescence emission under suitable conditions.<sup>65–71</sup> With RN-SPCL1 in  $\text{CH}_2\text{Cl}_2$  (20 mg/mL) as the representative, varying the excitation wavelength ( $\lambda_{\text{ex}}$ ) from 300 to 500 nm results in a significant red shift of the maximum emission

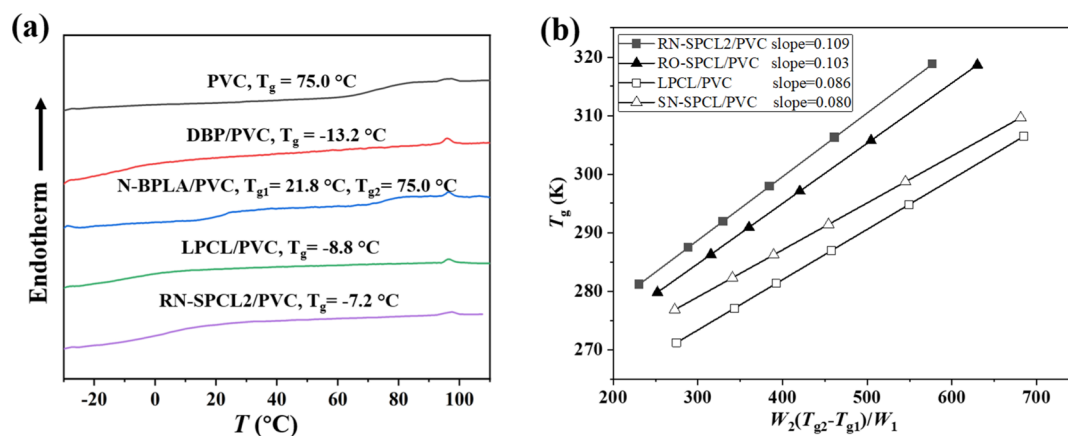


**Figure 3.** (a) Second-heating DSC thermograms of neat PVC and PVCs with 60 phr of different plasticizers; (b) Gordon–Taylor plots of composites of different PCL-based polymers with PVC.

wavelength ( $\lambda_{em,max}$ ) from 410 to 540 nm (Figures S7 and S8), implying the existence of different emitting species. RN-SPCL1 in  $CH_2Cl_2$  shows a maximum emission intensity at  $\lambda_{ex}$  of 365–375 nm and  $\lambda_{em}$  of 435–445 nm. From the excitation and emission fluorescence spectra of different concentrations of RN-SPCLs in  $CH_2Cl_2$  (Figure 1c), the RN-SPCLs show increased emission intensities and a slight red shift of  $\lambda_{ex,max}$  and  $\lambda_{em,max}$  upon raising the concentration from 2.0 to 20 mg/mL. On comparing with the emission spectra of RN-SPCLs at the same concentration, it can be found that RN-SPCL with more PCL content shows weaker emission (Figure 1d), ascribed to its lower nitrogen content. With quinine sulfate in 0.1 M  $H_2SO_4$  as the standard, the quantum yields of RN-SPCL1, RN-SPCL2, RN-SPCL3, RN-SPCL4, and RN-SPCL5 are measured to be 0.67%, 0.41%, 0.31%, 0.28%, and 0.25%, respectively (Figure S9).

**Formation of RN-SPCL/PVC Plastics.** RN-SPCL-containing PVC plastics are formed by casting the tetrahydrofuran (THF) solution containing both polymers in a polytetrafluoroethylene mold, followed by drying in an oven at 25 °C for 48 h, to form highly transparent films (Figure 2a). As shown by the Fourier-transform infrared spectroscopy (FT-IR) spectra in Figure 2b, the PVCs have characteristic bands at 2940, 1730, 1430, and 625  $cm^{-1}$ , corresponding to the C–H stretching, C=O stretching, C–H bending (methylene), and C–Cl stretching, respectively. LPCL/PVC and RN-SPCL2/PVC show an additional IR band at 1165  $cm^{-1}$ , corresponding to the C–O stretch of the ester group, whereas the C–O stretching band of DBP/PVC shifts to 1270  $cm^{-1}$  due to the aromatic group in DBP. As illustrated by the partial FT-IR spectra of the plasticizers and their corresponding PVC mixtures in the carbonyl region (Figures S10–S12), all the plasticizers show a significant shift of the C=O band after mixing with PVC due to the specific hydrogen-bonding interaction between the C=O groups in the plasticizer and the  $\alpha$ -hydrogen in PVC.<sup>72</sup> The efficient physical interaction between the plasticizer and PVC matrix confirmed by FT-IR spectra plays an important role in suppressing the crystallinity of PCLs and reducing the  $T_g$  of PVCs, improving the stretchability and toughness.

The low volatilities of plasticizers are also important for practical applications as high volatilities will pollute the environment and affect the mechanical performance. It can be seen from Figure 2c that RN-SPCLs in the PVC matrix show very low weight loss at 200 °C. After 60 min, only 11.3%

of RN-SPCLs and 17.0% of LPCL are volatilized, compared with 96.0% of weight loss for DBP under the same condition. This result indicates higher thermal stability of RN-SPCLs than DBP under the processing conditions. The migration stability of RN-SPCL/PVC plastics was also investigated by leaching tests conducted under harsh experimental conditions. This is important for plasticized PVC applied as packaging materials because the plasticizer may migrate out from the PVC matrix after exposing to oily foods, and the weight loss of PVC products caused by the plasticizer migration must not exceed 5.5%.<sup>17</sup> *n*-Hexane was selected as the extraction medium for plasticizer due to the fact that it readily swells PVC at a relatively high temperature and has a solubility profile similar to that of cooking oils. As shown in Figure 2d, the weight loss of DBP/PVC is 28.3%, much higher than the requirement, that is,  $\leq 5.5\%$  of weight loss. On the other hand, both LPCL- and RN-SPCL-plasticized PVCs can satisfy the requirement, whereas SPCLs show even lower weight loss than LPCL. The degree of plasticizer migration was calculated by measuring the specimen weight loss during the test period according to eq 1

$$\text{degree of plasticizer migration (\%)} = (W_1 - W_2) / (W_1 \times 60/100) \times 100 \quad (1)$$

where  $W_1$  and  $W_2$  represent the specimen weights before and after the tests, respectively.

As shown in Figure 2d, only a trace quantity of RN-SPCLs migrate out of the RN-SPCL/PVC specimens compared with a considerable quantity of DBP, that is, more than 75 wt % migrate out of the DBP/PVC specimens. The excellent migration resistance of RN-SPCLs in the RN-SPCL/PVC plastics can be explained by their high molecular weight and the presence of numerous carbonyl groups and hydroxyl groups that form efficient hydrogen bonding interactions with the  $\alpha$ -hydrogen and Cl-atom in PVC, respectively (Scheme 1b).<sup>25</sup> In addition, it can be seen from Figure S13 that the serious leaching of DBP results in significant increase of glass transition temperature ( $T_g$ ) for DBP/PVC, while the minor leaching of LPCL and RN-SPCLs will not significantly affect the  $T_g$  value of plasticized PVCs, especially for RN-SPCL-plasticized PVC.

**Thermal Property Analysis.** The efficiency of a typical plasticizer is mainly determined by its capability to endow targeting plastics with desired mechanical properties, such as

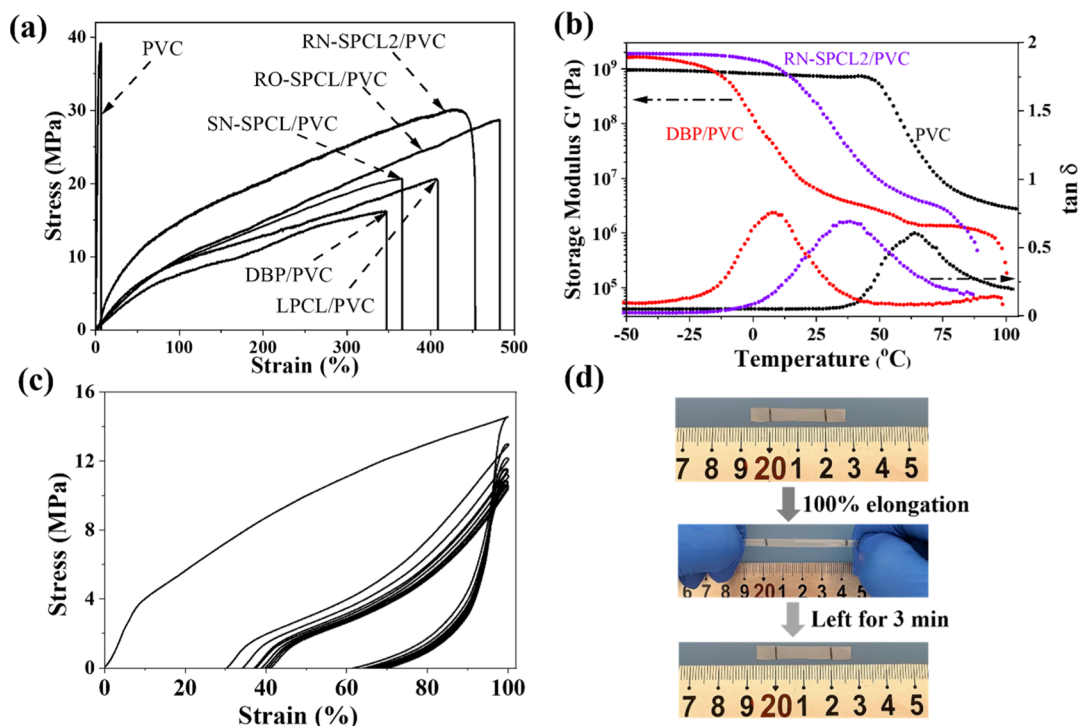


**Figure 4.** (a) Stress–strain curves of PVC and PVC-based elastomers, (b) temperature sweep of PVC, DBP/PVC, and RN-SPCL2/PVC using DMA, (c) 10 successive loading–unloading cycles of the films obtained from RN-SPCL2/PVC (films were pulled and released at a rate of  $0.5 \text{ mm s}^{-1}$  with an initial gauge length of 20 mm), (d) pictures showing the elongation and release of RN-SPCL2/PVC.

processability and flexibility, while such properties highly depend on their thermal state under service conditions.<sup>73</sup> Therefore, evaluating the thermal properties of resulting plastics, usually by thermogravimetric analysis (TGA) and DSC, is vital for evaluating plasticizer efficiency. The TGA thermograms (Figure S14) demonstrate the high thermal stability of RN-SPCL/PVC systems. The RN-SPCL2-plasticized PVCs have a similar onset decomposing temperature ( $T_{\text{onset}}$ ) to neat PVC and slightly higher temperature of maximum weight loss rate than neat PVC, which indicates the improved thermal stability of RN-SPCL-containing PVC. On the contrary, the conventional DBP plasticizer severely deteriorates the thermal stability of the PVC system. Meanwhile, DSC is used to measure the  $T_g$  of neat PVC and PVCs plasticized by the DBP, N-BPLA, LPCL, or RN-SPCLs. As illustrated by Figure 3a, even with 60 parts per hundred resins (phr) of plasticizers (*i.e.*, weight ratio of the plasticizer to PVC is 0.6), no crystallization peaks are observed from the PVC systems plasticized by semicrystalline LPCL and RN-SPCLs. Moreover, just like DBP-plasticized PVC, PVCs plasticized by 60 phr of LPCL and RN-SPCLs exhibit only one  $T_g$ . Both of these confirm the good compatibility of PCL-based polymers with PVCs due to the hydrogen-bonding interaction between the C=O groups in PCL and the  $\alpha$ -hydrogen in PVCs, as demonstrated in the FT-IR spectrum analysis (Figures S10–S12). On the other hand, the N-BPLA-plasticized PVC shows two  $T_g$  values, suggesting the incompatibility of the branched PLA with PVC.

With the  $T_g$  value higher than the room temperature, the neat PVCs are in a glassy state, which may be the primary reason for their low flexibility. Addition of 60 phr of DBP and LPCL enables the PVC systems with lower  $T_g$  values, that is,  $-13.2$  and  $-8.8$  °C, respectively. With moderate PCL length, the RN-SPCL2 shows the optimal plasticization efficiency

among synthesized RN-SPCLs, and the  $T_g$  of PVC can be lowered to  $-7.2$  °C by 60 phr of RN-SPCL2, achieving the transition from a glassy to rubbery state. According to the literature on hyperbranched plasticizers with a plenty of hydroxyl groups,<sup>23</sup> esterification of the hydroxyl groups with *n*-butyric acid ( $C_4$ ) can further lower the  $T_g$  of PVC. However, in our case, PVC plasticized by *n*-butyric acid-modified RN-SPCL2 shows a  $T_g$  of  $8.2$  °C (Figure S15), much higher than that of the unmodified plasticizer. This result points out the importance of terminal hydroxyl groups in the current SPCL plasticizer, which may contribute to their homogeneous dispersion into the PVC matrix through the hydrogen-bonding interactions between terminal OH groups of RN-SPCL and C–Cl units in PVC.

The effect of the N-BPLA core in the RN-SPCL2 is further studied by modifying the nitrogen-containing, rigid, branched PLA core (N-BPLA) to oxygen-containing, rigid, branched PLA (O-BPLA) or nitrogen-containing, flexible, branched PCL (N-BPCL), respectively (see comparative chemical structures in Figure S16). N-BPLA is an amorphous polymer with a  $T_g$  value of  $28.0$  °C. With similar rigidity to N-BPLA, the O-BPLA embodied with a slightly higher  $T_g$  of  $35.0$  °C, whereas N-BPCL is a comparatively softer core with a  $T_g$  of  $-57.5$  °C (Figure S17). RN-SPCL, RO-SPCL, and SN-SPCL are all semicrystalline polymers due to the existence of a strong melting peak in DSC thermograms (Figure S18), while with a softer core, the SN-SPCL is more prone to crystallize than RN-SPCL and RO-SPCL, embodied with a higher  $X_c$  value. Moreover, the soft N-BPCL core also results in the low  $T_g$  value of the resulting SN-SPCL ( $-64.1$  °C), which is similar to the  $T_g$  of LPCL ( $-65.1$  °C) and lower than those of RN-SPCL2 ( $T_g = -43.2$  °C) and RO-SPCL ( $T_g = -54.5$  °C). With 60 phr of semicrystalline RO-SPCL or SN-SPCL as the plasticizer, no crystallization peaks were observed in the DSC

**Table 1. Mechanical Properties of Neat PVC and Plasticized PVCs**

| no. | plasticizer | content of plasticizer (phr) <sup>a</sup> | <i>E</i> (MPa) <sup>b</sup> | $\sigma_b$ (MPa) <sup>c</sup> | $\epsilon_b$ (%) <sup>d</sup> | toughness (MJ/m <sup>3</sup> ) <sup>e</sup> |
|-----|-------------|---|-----------------------------|-------------------------------|-------------------------------|---|
| 1   | none        | 0   | 1209 ± 41                   | 39.2 ± 1.7                    | 6.5 ± 0.2                     | 1.8 ± 0.1                                   |
| 2   | DBP         | 60  | 9.3 ± 0.1                   | 16.3 ± 2.2                    | 348 ± 9                       | 34.7 ± 1.9                                  |
| 3   | LPCL        | 60  | 15.6 ± 0.6                  | 20.7 ± 1.4                    | 409 ± 13                      | 51.6 ± 1.8                                  |
| 4   | SN-SPCL     | 60  | 11.1 ± 0.4                  | 20.7 ± 1.6                    | 366 ± 16                      | 46.8 ± 2.4                                  |
| 5   | RO-SPCL     | 60  | 18.0 ± 0.8                  | 28.8 ± 2.5                    | 483 ± 17                      | 80.0 ± 4.1                                  |
| 6   | RN-SPCL2    | 60  | 48.2 ± 4.3                  | 30.1 ± 2.5                    | 453 ± 15                      | 92.7 ± 3.7                                  |
| 7   | RN-SPCL2    | 50  | 76.3 ± 6.3                  | 35.0 ± 2.7                    | 357 ± 10                      | 74.4 ± 2.8                                  |
| 8   | RN-SPCL2    | 10  | 1213 ± 55                   | 36.1 ± 2.5                    | 220 ± 6                       | 69.1 ± 1.5                                  |

<sup>a</sup>PVC is 100 phr. <sup>b</sup>*E* denotes Young's modulus. <sup>c</sup> $\sigma_b$  denotes tensile strength at break. <sup>d</sup> $\epsilon_b$  denotes elongation at break. <sup>e</sup>Tensile toughness is obtained from the integrated area under the stress–strain curve.

thermograms of the PVC systems, similar to RN-SPCL2/PVC and LPCL/PVC (Figure S19). Moreover, it can be found that SN-SPCL with a soft core can reduce  $T_g$  of PVC systems more efficiently than that of RN-SPCL2 or RO-SPCL with a hard core. The  $T_g$  of PVC systems can be reduced gradually through promoting the content of SPCL (Figure S19), and the data are fitted to the Gordon–Taylor equation (eq 2)<sup>74</sup>

$$T_g = T_{g1} + KW_2(T_{g2} - T_{g1})/W_1 \quad (2)$$

where 1 and 2 in this work represent PCL and PVC, respectively;  $W_i$  is the weight fraction of component *i*, and *K* is the Gordon–Taylor parameter that semiquantitatively demonstrates the interaction strength between two polymers.<sup>75</sup> As illustrated by the fitted data in Figure 3b, a clear linear relationship is observed for all PCL-based polymer-plasticized PVC, further indicating their good miscibility. From the slopes, *K* values are read off and they are 0.080, 0.086, 0.103, and 0.109 for SN-SPCL2/PVC, LPCL/PVC2/PVC, RO-SPCL2/PVC, and RN-SPCL2/PVC, respectively. These results imply that PVC has a stronger interaction with SPCLs having a rigid core, that is, RO-SPCL2 and RN-SPCL2, than the SPCL having a soft core and LPCLs. The different interactions between these PCL-based polymers and PVC might lead to the different mechanical properties of the obtained plasticized PVCs.

#### Mechanical Performance of RN-SPCL/PVC Plastics.

With a significantly reduced  $T_g$  value and transition from the “glassy” to “rubbery” state after addition of RN-SPCL, the mechanical performance of the RN-SPCL/PVC was also evaluated through the uniaxial tensile tests (Figure 4a). The tensile strength at break ( $\sigma_b$ ), elongation at break ( $\epsilon_b$ ), Young's modulus (*E*), and tensile toughness of neat PVC and PVC-based elastomers are summarized and listed in Table 1. With a high tensile strength and Young's modulus, the neat PVC only has an elongation before break of 6.5%, which is a relatively brittle material. The addition of a typical plasticizer, that is, DBP, to the PVC system affords improved elongation before breaks, that is, 348% while the Young's modulus and tensile strength are significantly sacrificed. Nevertheless, the overall toughness is still obviously improved from 1.8 to 34.7 MJ/m<sup>3</sup>. The dynamic mechanical analysis (DMA) of DBP/PVC, as illustrated in Figure 4b, manifests the drop of storage modulus (*E'*) at a significantly lower temperature compared with neat PVC, which also confirms the transition from the “glassy” to “rubbery” state at ambient temperature after the addition of DBP. The macromolecular plasticizer, that is, LPCL, shows enhanced plasticizing efficiency than DBP. The obtained LPCL/PVC achieves higher elongation before breaks, that is, 409% and more improved toughness, that is, 51.6 MJ/m<sup>3</sup> than

DBP/PVC. Combined with other benefits, such as high migration stability and thermal stability, it clearly demonstrates the significance of PCL-based plasticizers for PVC systems.

With the most efficient plasticization effect in lowering the  $T_g$  as demonstrated before, RN-SPCL2 has been selected for further mechanical studies. The RN-SPCL2/PVC not only shows more improved extensibility, that is, 453%, than those plasticized with DBP and LPCL but also maintains close to 80% of the tensile strength of neat PVC, that is, 30.1 MPa, which is much higher than the previously reported PCL-plasticized PVC systems (Table S2). Moreover, PVC plasticized by the as-prepared RN-SPCL2 possesses 3- to 5-fold higher Young's modulus than PVCs plasticized by DBP or LPCL. The overall toughness of the obtained RN-SPCL2/PVC was obtained, being 92.7 MJ/m<sup>3</sup>, more than 50-fold higher than neat PVC, and 2 to 3 times higher than LPCL- or DBP-plasticized PVCs (Table 1). The hysteresis of plasticized PVCs was measured through 10 successive cycles of loading and unloading processes in the elongation range of 0–100% at a rate of 0.8 mm s<sup>-1</sup> (Figures 4c and S20). Compared with DBP/PVC, the RN-SPCL2/PVC exhibits more leftover strain after 10 cycles of loading and unloading processes, that is, >40% for RN-SPCL2/PVC versus < 20% DBP/PVC (Figures 4c and S20). However, it is worth noticing that after 100% elongation and leaving for 3 min, the RN-SPCL2/PVC can almost completely return to its original length, as shown in Figure 4d (see Video S1 in the Supporting Information). This demonstrates that the RN-SPCL2/PVC also exhibits good elastic recovery while requiring longer relaxation time: 25 s of relaxation for 100% elongated films during the hysteresis test is not enough to recover their original length, and 3 min relaxation shown in the video will allow complete elastic recovery. The longer relaxation time required for RN-SPCL2/PVC than DBP/PVC can be explained by the fact that the high-molecular-weight RN-SPCL2 possesses much longer structure relaxation time compared with the low-molecular-weight DBP in the PVC matrix.<sup>76,77</sup>

Lowering the content of RN-SPCL2 will slightly reduce the elongation at breaks while markedly promoting the tensile strength and Young's modulus of the PVC-based elastomers. For instance, with the addition of 50 phr of RN-SPCL2, the prepared plasticized PVC has a similar extensibility with 60 phr of DBP plasticized PVC, 357% versus 348%. However, it can maintain close to 90% of the tensile strength of neat PVC, that is, 35.0 MPa, much superior to other reported plasticized PVCs with similar extensibility (see Table S2). By decreasing the amount of RN-SPCL2 to 10 phr, the as-prepared plasticized PVC still showed an elongation at break of 219%, that is, 35-fold higher than neat PVC, while maintaining the comparable

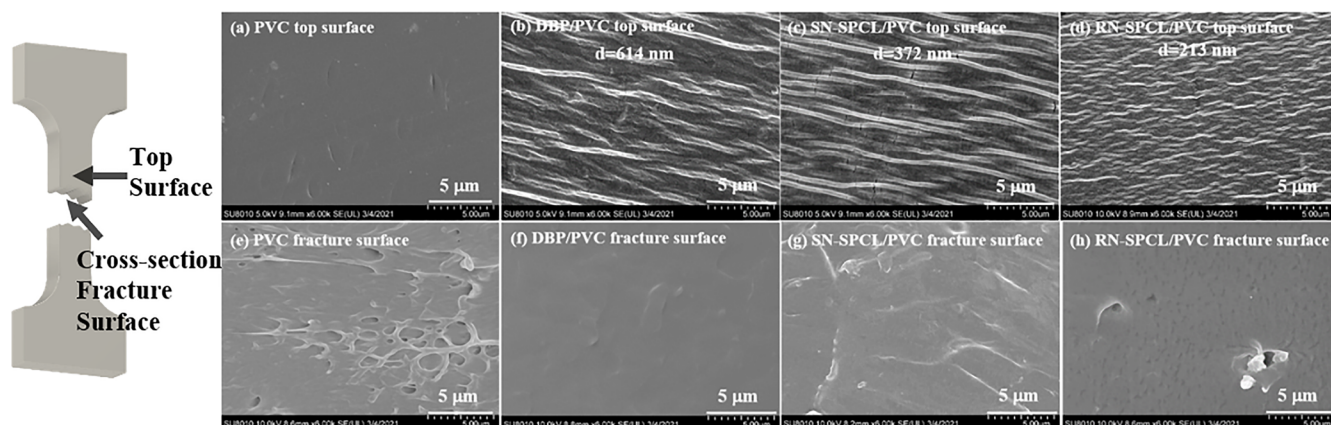


**Figure 5.** SEM micrographs of the top surface of fractured samples: (a) PVC; (b) DBP/PVC; (c) SN-SPCL/PVC; (d) RN-SPCL/PVC; and cross-sectional fracture surface of (e) PVC; (f) DBP/PVC; (g) SN-SPCL/PVC; (h) RN-SPCL/PVC.

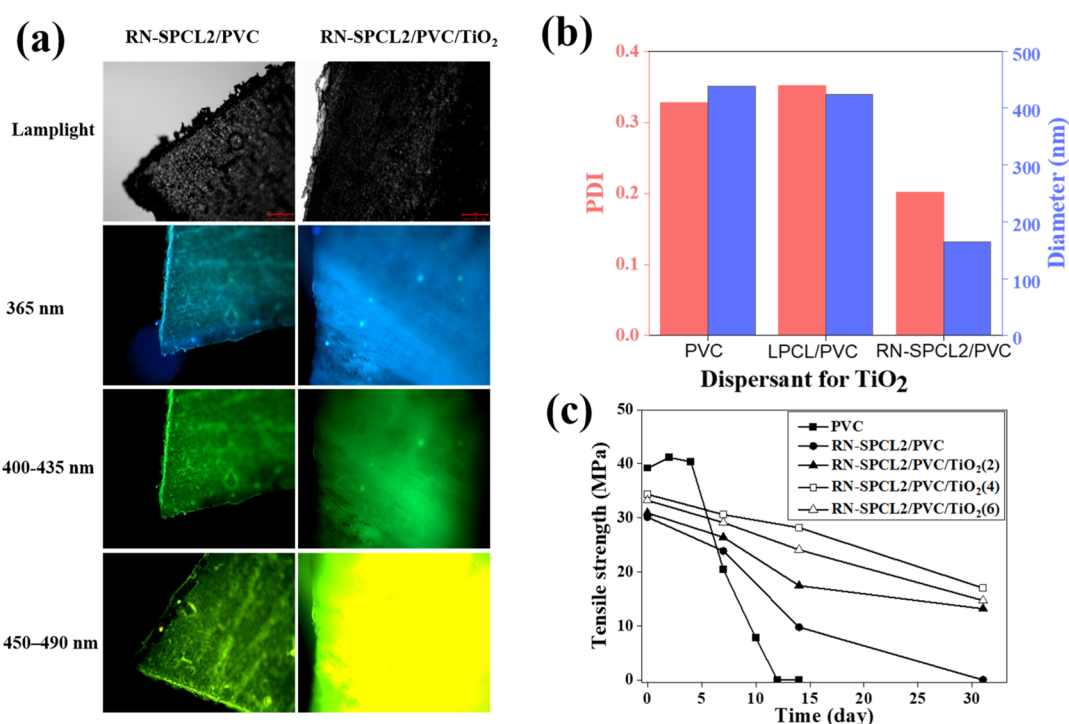


**Figure 6.** (a) Fluorescence imaging of RN-SPCL2-plasticized PVC and TiO<sub>2</sub>-doped RN-SPCL2-plasticized PVC under lamplight, 365, 400–435 and 450–490 nm excitation; (b) average diameter and polydispersity of TiO<sub>2</sub> in the PVC–THF solution with and without a dispersant; (c) mechanical properties of pristine PVC, RN-SPCL2/PVC, and TiO<sub>2</sub>-doped RN-SPCL2/PVCs under harsh UV irradiation for different times.

Young's modulus and tensile strength to neat PVC (Table 1). Overall, from the mechanical test, it can be deduced that RN-SPCL2 as a plasticizer can significantly improve the extensibility of PVCs systems while maintaining high tensile strength and Young's modulus.

The reason for achieving highly stretchable and ultratough PVC plastics with addition of RN-SPCL2 should be attributed to its unique core–shell structure with a relatively rigid BPLA core and many flexible PCL arms. The numerous flexible PCL arms in RN-SPCL2 can efficiently interact with PVC *via* suppressing the strong interaction among the polar C–Cl bonds (Scheme 1b), which can reduce the  $T_g$ , dissipate the energy of external forces, and significantly improve extensibility of PVC. More importantly, different from the previously reported linear or branched PCLs, the relatively rigid core should also allow RN-SPCL2 to serve as a strengthening agent

that improves the strength of PVC-based plastics, consistent with other nanofillers with a rigid core.<sup>78</sup> To test the assumption, the PVC plasticized by another star-shaped copolymer with a relatively rigid BPLA core, that is, RO-SPCL (chemical structure in Figure S16), was fabricated, and tensile test was conducted. The results show that the RO-SPCL/PVC also shows comparable extensibility and tensile strength with PVC/RN-SPCL, that is, 483% *versus* 453% and 28.8 MPa *versus* 30.1 MPa (Figure 4a). On the other hand, the PVC plasticized by the star-shaped copolymer with a flexible PCL core, that is, SN-SPCL, did not exhibit such high stretchability and strength, with overall toughness only around half of RN-SPCL/PVC, that is, 46.8 *versus* 92.7 MJ/m<sup>3</sup>. These facts demonstrate the essential role of a rigid core in SPCL in achieving highly stretchable, ultratough PVC plastics.

To further investigate the role of SN-SPCL in the mechanical performance of plasticized PVC, scanning electron microscopy (SEM) was also utilized to map the morphology of the film surface and cross-sectional fracture surface after the mechanical failure of PVC and plasticized PVCs (Figure 5). After the tensile test, unlike the neat PVC surface, all of the plasticized PVCs (Figure 5b–d) exhibited a fibril-like morphology with numerous fibrils vertical to the strain direction. This can be explained by the fact that the plasticizers can efficiently suppress the strong polar interaction of C–Cl bonds in bulk PVC (Scheme 1b) and disassemble them into bundles of fibrils. The comparatively lower average diameters of formed fibrils in RN-SPCL/PVC compared with DBP/PVC and SN-SPCL/PVC (213 nm vs 614 and 372 nm) manifest the improved compatibility of RN-SPCL to PVC than the others. More interestingly, compared with the relatively smooth surface observed from the cross-sectional fracture surfaces of DBP/PVC and SN-SPCL/PVC (Figure 5f,g), the fracture surfaces formed by neat PVC and RN-SPCL/PVC characteristic of high breaking stress are rugged with some voids (Figure 5e,h). Especially, compared with PVC plasticized by SPCL possessing a soft core, that is, SN-SPCL, the formation of a myriad of nanocavities derived from that with a rigid core, that is, RN-SPCL/PVC, manifests the additional cavitation mechanism during the uniaxial deformation process. These results demonstrated the additional role of RN-SPCL2 in PVC plastics that act as an *in situ* “bridge” over the crazes/cavitation and hence resist the craze growth and contribute to the highly stretchable and ultratough PVC plastics.<sup>79</sup>

**Functionalities of RN-SPCL/PVC Plastics.** Aside from significantly improved extensibility and toughness, the obtained RN-SPCL/PVC also shows other unique functionalities due to the core–shell structured copolymers with the relatively rigid amino-containing core. First, the RN-SPCL endows the PVC elastomers with photoluminescence nature. With intrinsic photoluminescence emission of the prepared amino-containing RN-SPCLs under suitable conditions as demonstrated before, the emission properties of the formed PVC elastomers were also investigated. As shown in Figure 6a, under UV light irradiation, that is, wavelength 365 nm, the RN-SPCL2/PVC film can emit cyan light, and under the visible light irradiations, that is, wavelength of 400–435 nm and 450–490 nm, it can result in green light emission. On the contrary, the neat PVC and LPCL/PVC do not show photoluminescence emission under the same light irradiation (Figure S22). This demonstrates the important role of tertiary amine groups in the effective photoluminescence properties of the as-prepared PVC elastomers.

At the same time, the RN-SPCL can act as an efficient dispersant of TiO<sub>2</sub> nanoparticles, which can significantly improve the anti-UV aging capability of PVC plastics. The nanosized TiO<sub>2</sub> is a well-known anti-UV aging material, and it is usually blended with PVC through the solution method. However, during this process, some TiO<sub>2</sub> granules precipitate immediately once the ultrasonic or mechanical mixing stops, implying the poor compatibility between TiO<sub>2</sub> nanoparticles and the PVC matrix.<sup>80,81</sup> In the current design, stable dispersion of TiO<sub>2</sub> could be acquired when RN-SPCL2 is present. After ultrasonic treatment for more than half an hour, the average particle size and polydispersity index (PDI) acquired from dynamic light scattering (DLS) were found to reach a minima of ca. 165 nm and 0.23, respectively (Figure 6b). On the contrary, the average particle size and PDI become

ca. 420 nm and 0.35, respectively, when using the same amount of LPCL, which are close to the data found for the mixture of TiO<sub>2</sub> and PVC in THF. These results imply that the RN-SPCL can act as an efficient dispersant for the homogeneous dispersion of TiO<sub>2</sub> nanoparticles into the PVC matrix, while the LPCL cannot.

To further test the UV-aging properties of the obtained PVC plastics, RN-SPCL2/PVCs doped with 2, 4, and 6 phr of TiO<sub>2</sub> were prepared and compared with the pristine PVC and RN-SPCL2/PVC under harsh UV irradiation (150 W UV lamp with a 365 nm light). DSC tests of the samples after UV irradiation demonstrate a significant role of doped nano-TiO<sub>2</sub>: without the addition TiO<sub>2</sub>, the  $T_g$  of RN-SPCL2/PVC increases significantly from the original  $-7.2$  to  $51.2$  °C after 31-day UV aging, whereas the films doped with 2, 4, and 6 phr of TiO<sub>2</sub> show  $T_g$  of 7.0, 8.6, and 7.9 °C, respectively, after the same process. The tensile test shows that the RN-SPCL2/PVC elastomers lose around 67% tensile strength and 90% elongation at break after 14-day UV aging compared with the pristine PVC, which almost completely lost its tensile strength after 12 days (Figures 6c and S23). The RN-SPCL2/PVCs with doped TiO<sub>2</sub> shows significantly improved anti-UV aging performance, that is, maintaining 50% of tensile strength and elongation at break even after 31-day aging. The above tests on the variation of thermal property and mechanical performance during the UV aging demonstrate the enhanced anti-UV ability of RN-SPCL2/PVCs, especially after doping with nanosized TiO<sub>2</sub>.

## CONCLUSIONS

A series of highly stretchable and ultratough PVC-based plastics were successfully prepared by addition of a SPCL plasticizer with a rigid, amino-containing, branched PLA (N-BPLA) core and a soft PCL shell, that is, RN-SPCLs. From the hydroxyl-terminated hyperbranched PLA, ring-opening polymerization of the CL monomer affords RN-SPCLs with tunable arm lengths. As a “green” plasticizer, the RN-SPCLs shows low volatility and excellent migration resistance in the PVC matrix. Such RN-SPCLs increased the extensibility of PVC more efficiently than PCLs with other topologies, including linear/star-shaped with a soft core and low-molecular-weight conventional plasticizer, DBP. The RN-SPCL2/PVC shows improved extensibility, that is, 453%, high tensile strength, that is, 30.1 MPa and ultrahigh overall toughness, that is, 92.7 MJ/m<sup>3</sup>, more than 50-fold higher than neat PVC and 2 to 3 times higher LPCL- or DBP-plasticized PVC. It was demonstrated that the relatively rigid core in the SPCLs should also allow RN-SPCL2 to serve as the strengthening agent and act as an *in situ* “bridge” over the crazes/cavitation, contributing to the highly stretchable and ultratough PVC plastics. Moreover, RN-SPCLs also afford extra characteristics to PVC-based elastomers: endowing photoluminescence property and helping nanosized TiO<sub>2</sub> to disperse homogeneously into the PVC matrix for enhanced anti-UV ability.

It is worth noticing that the star-shaped structure with a relatively rigid core plays an important role in their mechanical performance improvement, and the amino-containing branched PLAs allow extra capability to PVC plastics. This study not only reports a highly tough elastic material that can benefit a wide range of applications, including stretchable devices/electronics, food packaging, and medical devices, but also elaborates structure design on the high-performance,

“green” plasticizer, providing useful guidance for achieving other types of elastic materials.

## ■ ASSOCIATED CONTENT

### SI Supporting Information

The Supporting Information is available free of charge at <https://pubs.acs.org/doi/10.1021/acs.macromol.1c00029>.

<sup>1</sup>H NMR spectra of unpurified and purified polymers; UV–vis, IR and fluorescence spectra, DSC thermograms, POM images, TGA, DLS of copolymers (PDF) Five cycles of stretch and release of RN-SPCL2/PVC (MP4)

## ■ AUTHOR INFORMATION

### Corresponding Authors

**Yu Chen** – Department of Chemistry, School of Science, Tianjin University, Tianjin 300354, P. R. China; Tianjin Engineering Technology Center of Chemical Wastewater Source Reduction and Recycling, School of Science, Tianjin Chengjian University, Tianjin 300384, P. R. China; [orcid.org/0000-0002-0559-6136](https://orcid.org/0000-0002-0559-6136); Email: [chenyu@tju.edu.cn](mailto:chenyu@tju.edu.cn)

**Peng-Fei Cao** – Chemical Sciences Division, Oak Ridge National Laboratory, Oak Ridge, Tennessee 37830, United States; [orcid.org/0000-0003-2391-1838](https://orcid.org/0000-0003-2391-1838); Email: [caop@ornl.gov](mailto:caop@ornl.gov)

### Authors

**Wei-Guang Chen** – Department of Chemistry, School of Science, Tianjin University, Tianjin 300354, P. R. China

**Hai-Jie Wei** – Department of Chemistry, School of Science, Tianjin University, Tianjin 300354, P. R. China

**Jiancheng Luo** – Chemical Sciences Division, Oak Ridge National Laboratory, Oak Ridge, Tennessee 37830, United States; [orcid.org/0000-0002-3766-4922](https://orcid.org/0000-0002-3766-4922)

Complete contact information is available at:

<https://pubs.acs.org/doi/10.1021/acs.macromol.1c00029>

### Notes

The authors declare no competing financial interest.

## ■ ACKNOWLEDGMENTS

This work was financially supported by the National Natural Science Foundation of China (21875159) and Natural Science Foundation of Tianjin City (18JCYBJC86800). P.-F. Cao also acknowledges partial financial support on idea conception and manuscript revision by the US Department of Energy, Office of Science, Basic Energy Science, Material Science, and Engineering Division for manuscript conceptualization and revision.

## ■ REFERENCES

- (1) Wang, C.; Wang, C.; Huang, Z.; Xu, S. Materials and Structures toward Soft Electronics. *Adv. Mater.* **2018**, *30*, 1801368.
- (2) Xu, Z.; Chen, L.; Lu, L.; Du, R.; Ma, W.; Cai, Y.; An, X.; Wu, H.; Luo, Q.; Xu, Q.; Zhang, Q.; Jia, X. A Highly-Adhesive and Self-Healing Elastomer for Bio-Interfacial Electrode. *Adv. Funct. Mater.* **2021**, *31*, 2006432.
- (3) Shi, Y.; Liu, C.; Duan, Z.; Yu, B.; Liu, M.; Song, P. Interface engineering of MXene towards super-tough and strong polymer nanocomposites with high ductility and excellent fire safety. *Chem. Eng. J.* **2020**, *399*, 125829.
- (4) Zhang, Z.; Ghezawi, N.; Li, B.; Ge, S.; Zhao, S.; Saito, T.; Hun, D.; Cao, P. F. Autonomous Self-Healing Elastomers with

Unprecedented Adhesion Force. *Adv. Funct. Mater.* **2021**, *31*, 2006298.

(5) Mannsfeld, S. C. B.; Tee, B. C.-K.; Stoltenberg, R. M.; Chen, C. V. H.-H.; Barman, S.; Muir, B. V. O.; Sokolov, A. N.; Reese, C.; Bao, Z. Highly sensitive flexible pressure sensors with microstructured rubber dielectric layers. *Nat. Mater.* **2010**, *9*, 859–864.

(6) Zhou, G.; Li, F.; Cheng, H.-M. Progress in flexible lithium batteries and future prospects. *Energy Environ. Sci.* **2014**, *7*, 1307–1338.

(7) Koo, J. H.; Kim, D. C.; Shim, H. J.; Kim, T.-H.; Kim, D.-H. Flexible and Stretchable Smart Display: Materials, Fabrication, Device Design, and System Integration. *Adv. Funct. Mater.* **2018**, *28*, 1801834.

(8) Li, Y.; Li, W.; Sun, A.; Jing, M.; Liu, X.; Wei, L.; Wu, K.; Fu, Q. A self-reinforcing and self-healing elastomer with high strength, unprecedented toughness and room-temperature reparability. *Mater. Horiz.* **2021**, *8*, 267–275.

(9) DeButts, B. L.; Chauhan, N.; Barone, J. R. Agricultural proteins as multifunctional additives in ZnO-free synthetic isoprene rubber vulcanizates. *J. Appl. Polym. Sci.* **2019**, *136*, 48141.

(10) Wen, H.-F.; Wu, H.-C.; Aimi, J.; Hung, C.-C.; Chiang, Y.-C.; Kuo, C.-C.; Chen, W.-C. Soft Poly(butyl acrylate) Side Chains toward Intrinsically Stretchable Polymeric Semiconductors for Field-Effect Transistor Applications. *Macromolecules* **2017**, *50*, 4982–4992.

(11) Cao, P.-F.; Li, B.; Hong, T.; Xing, K.; Voylov, D. N.; Cheng, S.; Yin, P.; Kisluk, A.; Mahurin, S. M.; Sokolov, A. P.; Saito, T. Robust and Elastic Polymer Membranes with Tunable Properties for Gas Separation. *ACS Appl. Mater. Interfaces* **2017**, *9*, 26483–26491.

(12) Breuillac, A.; Kassalias, A.; Nicolaj, R. Polybutadiene Vitrimers Based on Dioxaborolane Chemistry and Dual Networks with Static and Dynamic Cross-links. *Macromolecules* **2019**, *52*, 7102–7113.

(13) Cao, P.-F.; Li, B.; Hong, T.; Townsend, J.; Qiang, Z.; Xing, K.; Vogiatzis, K. D.; Wang, Y.; Mays, J. W.; Sokolov, A. P.; Saito, T. Superstretchable, Self-Healing Polymeric Elastomers with Tunable Properties. *Adv. Funct. Mater.* **2018**, *28*, 1800741.

(14) Li, H.; Thanneer, S.; Jin, L.; Guild, C. J.; He, J. Multiblock thermoplastic elastomers via one-pot thiol-ene reaction. *Polym. Chem.* **2016**, *7*, 4824–4832.

(15) Li, B.; Zhao, S.; Zhu, J.; Ge, S.; Xing, K.; Sokolov, A. P.; Saito, T.; Cao, P.-F. Rational Polymer Design of Stretchable Poly(ionic liquid) Membranes for Dual Applications. *Macromolecules* **2021**, *54*, 896–905.

(16) Wang, W.; Lu, W.; Goodwin, A.; Wang, H.; Yin, P.; Kang, N.-G.; Hong, K.; Mays, J. W. Recent advances in thermoplastic elastomers from living polymerizations: Macromolecular architectures and supramolecular chemistry. *Prog. Polym. Sci.* **2019**, *95*, 1–31.

(17) Choi, W.; Chung, J. W.; Kwak, S.-Y. Unentangled Star-Shape Poly( $\epsilon$ -caprolactone)s as Phthalate-Free PVC Plasticizers Designed for Non-Toxicity and Improved Migration Resistance. *ACS Appl. Mater. Interfaces* **2014**, *6*, 11118–11128.

(18) Raeisi, A.; Allahyari, F.; Faghihi, K.; Hosseini-Ghazvini, S. M.-B.; Khaleghi, M.; Seidi, F.; Shabani, M. A complete description on effect of  $\beta$ -cyclodextrin-ester as a bio-based additive for preparation of safe PVC: From synthesis to computational study. *Mater. Today Commun.* **2020**, *22*, 100736.

(19) Sun, Z.; Choi, B.; Feng, A.; Moad, G.; Thang, S. H. Nonmigratory Poly(vinyl chloride)-block-polycaprolactone Plasticizers and Compatibilizers Prepared by Sequential RAFT and Ring-Opening Polymerization (RAFT-T-ROP). *Macromolecules* **2019**, *52*, 1746–1756.

(20) Saeki, Y.; Emura, T. Technical progresses for PVC production. *Prog. Polym. Sci.* **2002**, *27*, 2055–2131.

(21) Braun, D. Poly(vinyl chloride) on the Way from the 19th Century to the 21st Century. *J. Polym. Sci., Part A: Polym. Chem.* **2004**, *42*, 578–586.

(22) Moulay, S. Chemical modification of poly(vinyl chloride)-Still on the run. *Prog. Polym. Sci.* **2010**, *35*, 303–331.

(23) Lee, K. W.; Chung, J. W.; Kwak, S.-Y. Highly Branched Polycaprolactone/Glycidol Copolymeric Green Plasticizer by One-

Pot Solvent-Free Polymerization. *ACS Sustainable Chem. Eng.* **2018**, *6*, 9006–9017.

(24) Li, W.; Qin, J.; Wang, S.; Han, D.; Xiao, M.; Meng, Y. Macrodiols Derived from CO<sub>2</sub>-Based Polycarbonate as an Environmentally Friendly and Sustainable PVC Plasticizer: Effect of Hydrogen-Bond Formation. *ACS Sustainable Chem. Eng.* **2018**, *6*, 8476–8484.

(25) Daniels, P. H. A brief overview of theories of PVC plasticization and methods used to evaluate PVC-plasticizer interaction. *J. Vinyl Addit. Technol.* **2009**, *15*, 219–223.

(26) Rahman, M.; Brazel, C. The plasticizer market: an assessment of traditional plasticizers and research trends to meet new challenges. *Prog. Polym. Sci.* **2004**, *29*, 1223–1248.

(27) Kumar, S. Recent Developments of Biobased Plasticizers and Their Effect on Mechanical and Thermal Properties of Poly(vinyl chloride): A Review. *Ind. Eng. Chem. Res.* **2019**, *58*, 11659–11672.

(28) Janjua, N. R.; Mortensen, G. K.; Andersson, A.-M.; Kongshoj, B.; Skakkebæk, N. E.; Wulf, H. C. Systemic Uptake of Diethyl Phthalate, Dibutyl Phthalate, and Butyl Paraben Following Whole-Body Topical Application and Reproductive and Thyroid Hormone Levels in Humans. *Environ. Sci. Technol.* **2007**, *41*, 5564–5570.

(29) Heudorf, U.; Mersch-Sundermann, V.; Angerer, J. Phthalates: Toxicology and exposure. *Int. J. Hyg. Environ. Health* **2007**, *210*, 623–634.

(30) Gao, C.; Wang, B.; Hu, Z.; Liu, Y.; Wang, H.; Zhang, X.; Wu, Y. Effect of the molecular weight on the plasticization properties of poly(hexane succinate) in poly(vinyl chloride) blends. *J. Appl. Polym. Sci.* **2019**, *136*, 47081.

(31) Jia, P.; Bo, C.; Hu, L.; Zhang, M.; Zhou, Y. Synthesis of a novel polyester plasticizer based on glyceryl monooleate and its application in poly(vinyl chloride). *J. Vinyl Addit. Technol.* **2016**, *22*, 514–519.

(32) Xie, T.; Gao, C.; Wang, C.; Shen, S. e.; Wu, Y. Application of Poly(butylene 2-methylsuccinate) as Migration Resistant Plasticizer for Poly(vinyl chloride). *Polym.-Plast. Technol. Eng.* **2014**, *53*, 465–471.

(33) Ferruti, P.; Mancin, I.; Ranucci, E.; De Felice, C.; Latini, G.; Laus, M. Polycaprolactone–Poly(ethylene glycol) Multiblock Copolymers as Potential Substitutes for Di(ethylhexyl) Phthalate in Flexible Poly(vinyl chloride) Formulations. *Biomacromolecules* **2003**, *4*, 181–188.

(34) Lee, K. W.; Chung, J. W.; Kwak, S.-Y. Synthesis and characterization of bio-based alkyl terminal hyperbranched polyglycerols: a detailed study of their plasticization effect and migration resistance. *Green Chem.* **2016**, *18*, 999–1009.

(35) Jia, P.; Ma, Y.; Zhang, M.; Hu, L.; Zhou, Y. Designing Rosin-Based Plasticizers: Effect of Differently Branched Chains on Plasticization Performance and Solvent Resistance of Flexible Poly(vinyl chloride) Films. *ACS Omega* **2019**, *4*, 3178–3187.

(36) Yang, Y.; Huang, J.; Zhang, R.; Zhu, J. Designing bio-based plasticizers: Effect of alkyl chain length on plasticization properties of isosorbide diesters in PVC blends. *Mater. Des.* **2017**, *126*, 29–36.

(37) Pyeon, H. B.; Park, J. E.; Suh, D. H. Non-phthalate plasticizer from camphor for flexible PVC with a wide range of available temperature. *Polym. Test.* **2017**, *63*, 375–381.

(38) Jia, P.; Zhang, M.; Hu, L.; Feng, G.; Bo, C.; Zhou, Y. Synthesis and Application of Environmental Castor Oil Based Polyol Ester Plasticizers for Poly(vinyl chloride). *ACS Sustainable Chem. Eng.* **2015**, *3*, 2187–2193.

(39) Rahman, M.; Brazel, C. S. Ionic liquids: New generation stable plasticizers for poly(vinyl chloride). *Polym. Degrad. Stab.* **2006**, *91*, 3371–3382.

(40) Yin, B.; Hakkarainen, M. Oligomeric Isosorbide Esters as Alternative Renewable Resource Plasticizers for PVC. *J. Appl. Polym. Sci.* **2011**, *119*, 2400–2407.

(41) Chen, J.; Liu, Z.; Jiang, J.; Nie, X.; Zhou, Y.; Murray, R. E. A novel biobased plasticizer of epoxidized cardanol glycidyl ether: synthesis and application in soft poly(vinyl chloride) films. *RSC Adv.* **2015**, *5*, 56171–56180.

(42) Stuart, A.; LeCaptain, D. J.; Lee, C. Y.; Mohanty, D. K. Poly(vinyl chloride) plasticized with mixtures of succinate di-esters - synthesis and characterization. *Eur. Polym. J.* **2013**, *49*, 2785–2791.

(43) Wang, M.; Song, X.; Jiang, J.; Xia, J.; Ding, H.; Li, M. Plasticization and thermal behavior of hydroxyl and nitrogen rich group-containing tung-oil-based ester plasticizers for PVC. *New J. Chem.* **2018**, *42*, 2422–2431.

(44) Yin, B.; Aminlashgari, N.; Yang, X.; Hakkarainen, M. Glucose esters as biobased PVC plasticizers. *Eur. Polym. J.* **2014**, *58*, 34–40.

(45) Feng, G.; Hu, L.; Ma, Y.; Jia, P.; Hu, Y.; Zhang, M.; Liu, C.; Zhou, Y. An efficient bio-based plasticizer for poly(vinyl chloride) from waste cooking oil and citric acid: Synthesis and evaluation in PVC films. *J. Cleaner Prod.* **2018**, *189*, 334–343.

(46) Saltos, J. A.; Shi, W.; Mancuso, A.; Sun, C.; Park, T.; Averick, N.; Punia, K.; Fata, J.; Raja, K. Curcumin-derived green plasticizers for poly(vinyl chloride). *RSC Adv.* **2014**, *4*, 54725–54728.

(47) Suzuki, A. H.; Botelho, B. G.; Oliveira, L. S.; Franca, A. S. Sustainable synthesis of epoxidized waste cooking oil and its application as a plasticizer for polyvinyl chloride films. *Eur. Polym. J.* **2018**, *99*, 142–149.

(48) Mukherjee, S.; Ghosh, M. Studies on performance evaluation of a green plasticizer made by enzymatic esterification of furfuryl alcohol and castor oil fatty acid. *Carbohydr. Polym.* **2017**, *157*, 1076–1084.

(49) Omrani, I.; Ahmadi, A.; Farhadian, A.; Shendi, H. K.; Babanejad, N.; Nabid, M. R. Synthesis of a bio-based plasticizer from oleic acid and its evaluation in PVC formulations. *Polym. Test.* **2016**, *56*, 237–244.

(50) Bocqué, M.; Voirin, C.; Lapinte, V.; Caillol, S.; Robin, J.-J. Petro-Based and Bio-Based Plasticizers: Chemical Structures to Plasticizing Properties. *J. Polym. Sci., Part A: Polym. Chem.* **2016**, *54*, 11–33.

(51) Jia, P.; Xia, H.; Tang, K.; Zhou, Y. Plasticizers Derived from Biomass Resources: A Short Review. *Polymers* **2018**, *10*, 1303.

(52) Chiu, F.-C.; Min, K. Miscibility, morphology and tensile properties of vinyl chloride polymer and poly( $\epsilon$ -caprolactone) blends. *Polym. Int.* **2000**, *49*, 223–234.

(53) Shi, G.; Cooper, D. G.; Maric, M. Poly( $\epsilon$ -caprolactone)-based 'green' plasticizers for poly(vinyl chloride). *Polym. Degrad. Stab.* **2011**, *96*, 1639–1647.

(54) Cao, P.-F.; Mangadla, J. D.; de Leon, A.; Su, Z.; Advincula, R. C. Catenated Poly( $\epsilon$ -caprolactone) and Poly(l-lactide) via Ring-Expansion Strategy. *Macromolecules* **2015**, *48*, 3825–3833.

(55) Cao, P.-F.; Mangadla, J.; Advincula, R. A Trefoil Knotted Polymer Produced through Ring Expansion. *Angew. Chem., Int. Ed.* **2015**, *54*, 5127–5131.

(56) Wang, Y.; Li, K.; Zhao, X.; Tekinalp, H.; Li, T.; Ozcan, S. Toughening by Nanodroplets: Polymer-Droplet Biocomposite with Anomalous Toughness. *Macromolecules* **2020**, *53*, 4568–4576.

(57) Huang, Y.; Yu, E.; Li, Y.; Wei, Z. Novel branched poly( $\epsilon$ -caprolactone) as a nonmigrating plasticizer in flexible PVC: synthesis and characterization. *J. Appl. Polym. Sci.* **2018**, *135*, 46542.

(58) Choi, J.; Kwak, S.-Y. Hyperbranched Poly( $\epsilon$ -caprolactone) as a Nonmigrating Alternative Plasticizer for Phthalates in Flexible PVC. *Environ. Sci. Technol.* **2007**, *41*, 3763–3768.

(59) Li, Y.; Yu, E.; Yang, X.; Wei, Z. Multiarm hyperbranched polyester-b-Poly( $\epsilon$ -caprolactone): Plasticization effect and migration resistance for PVC. *J. Vinyl Addit. Technol.* **2020**, *26*, 35–42.

(60) Labet, M.; Thielemans, W. Synthesis of polycaprolactone: a review. *Chem. Soc. Rev.* **2009**, *38*, 3484–3504.

(61) Aubin, M.; Prud'homme, R. E. Analysis of the Glass Transition Temperature of Miscible Polymer Blends. *Macromolecules* **1988**, *21*, 2945–2949.

(62) Buntara, T.; Noel, S.; Phua, P. H.; Melián-Cabrera, I.; de Vries, J. G.; Heeres, H. J. Caprolactam from Renewable Resources: Catalytic Conversion of 5-Hydroxymethylfurfural into Caprolactone. *Angew. Chem.* **2011**, *123*, 7221–7225.

(63) Chen, W.-G.; Hu, N.; Chen, Y.; Pan, H. Sustainable branched polyactides with N,N-bis(2-hydroxyethyl)glycine as branching units:

Intrinsic photoluminescence, guest encapsulation and multifunctional additive for poly(l-lactide) plastics. *Polymer* **2020**, *196*, 122484.

(64) Fieber, W.; Herrmann, A.; Ouali, L.; Velazco, M. I.; Kreutzer, G.; Klok, H.-A.; Ternat, C.; Plummer, C. J. G.; Manson, J.-A. E.; Sommer, H. NMR Diffusion and Relaxation Studies of the Encapsulation of Fragrances by Amphiphilic Multiarm Star Block Copolymers. *Macromolecules* **2007**, *40*, 5372–5378.

(65) Liu, M.-N.; Chen, W.-G.; Liu, H.-J.; Chen, Y. Facile synthesis of intrinsically photoluminescent hyperbranched polyethylenimine and its specific detection for copper ion. *Polymer* **2019**, *172*, 110–116.

(66) Yang, W.; Pan, C.-Y. Synthesis and Fluorescent Properties of Biodegradable Hyperbranched Poly(amido amine)s. *Macromol. Rapid Commun.* **2009**, *30*, 2096–2101.

(67) Zhan, C.; Fu, X.-B.; Yao, Y.; Liu, H.-J.; Chen, Y. Stimuli-responsive hyperbranched poly(amidoamine)s integrated with thermal and pH sensitivity, reducible degradability and intrinsic photoluminescence. *RSC Adv.* **2017**, *7*, 5863–5871.

(68) Wang, P.; Wang, X.; Meng, K.; Hong, S.; Liu, X.; Cheng, H.; Han, C. C. Thermal sensitive fluorescent hyperbranched polymer without fluorophores. *J. Polym. Sci., Part A: Polym. Chem.* **2008**, *46*, 3424–3428.

(69) Fan, Y.; Cai, Y.-Q.; Fu, X.-B.; Yao, Y.; Chen, Y. Core-shell type hyperbranched grafting copolymers: Preparation, characterization and investigation on their intrinsic fluorescence properties. *Polymer* **2016**, *107*, 154–162.

(70) Pastor-Pérez, L.; Chen, Y.; Shen, Z.; Lahoz, A.; Stiriba, S.-E. Unprecedented Blue Intrinsic Photoluminescence from Hyperbranched and Linear Polyethylenimines: Polymer Architectures and pH-Effects. *Macromol. Rapid Commun.* **2007**, *28*, 1404–1409.

(71) Dai, Y.-X.; Lv, F.-N.; Wang, B.; Chen, Y. Thermoresponsive phenolic formaldehyde amines with strong intrinsic photoluminescence: Preparation, characterization and application as hardeners in waterborne epoxy resin formulations. *Polymer* **2018**, *145*, 454–462.

(72) Coleman, M. M.; Zarian, J. Fourier-transform infrared studies of polymer blends. II. Poly(*ε*-caprolactone)–poly(vinyl chloride) system. *J. Polym. Sci., Polym. Phys. Ed.* **1979**, *17*, 837–850.

(73) Cao, P.-F.; Li, B.; Yang, G.; Zhao, S.; Townsend, J.; Xing, K.; Qiang, Z.; Vogiatzis, K. D.; Sokolov, A. P.; Nanda, J.; Saito, T. Elastic Single-Ion Conducting Polymer Electrolytes: Toward a Versatile Approach for Intrinsically Stretchable Functional Polymers. *Macromolecules* **2020**, *53*, 3591–3601.

(74) Gordon, M.; Taylor, J. S. Ideal copolymers and the second-order transitions of synthetic rubbers. i. non-crystalline copolymers. *J. Appl. Chem.* **1952**, *2*, 493–500.

(75) BÉlorgey, G.; Aubin, M.; Prud'homme, R. E. Studies of polyester/chlorinated poly(vinyl chloride) blends. *Polymer* **1982**, *23*, 1051–1056.

(76) Tarnacka, M.; Talik, A.; Kamińska, E.; Geppert-Rybczyńska, M.; Kaminski, K.; Paluch, M. The Impact of Molecular Weight on the Behavior of Poly(propylene glycol) Derivatives Confined within Alumina Templates. *Macromolecules* **2019**, *52*, 3516–3529.

(77) Xing, K.; Tress, M.; Cao, P.-F.; Fan, F.; Cheng, S.; Saito, T.; Sokolov, A. P. The Role of Chain-End Association Lifetime in Segmental and Chain Dynamics of Telechelic Polymers. *Macromolecules* **2018**, *51*, 8561–8573.

(78) Sun, Y.; Ma, Z.; Xu, X.; Liu, X.; Liu, L.; Huang, G.; Liu, L.; Wang, H.; Song, P. Grafting Lignin with Bioderived Polyacrylates for Low-Cost, Ductile, and Fully Biobased Poly(lactic acid) Composites. *ACS Sustainable Chem. Eng.* **2020**, *8*, 2267–2276.

(79) Sun, Y.; Fan, X.; Lu, X.; He, C. Overcome the Conflict between Strength and Toughness in Poly(lactide) Nanocomposites through Tailoring Matrix-Filler Interface. *Macromol. Rapid Commun.* **2019**, *40*, No. e1800047.

(80) Rabiee, H.; Farahani, M. H. D. A.; Vatanpour, V. Preparation and characterization of emulsion poly(vinyl chloride) (EPVC)/TiO<sub>2</sub> nanocomposite ultrafiltration membrane. *J. Membr. Sci.* **2014**, *472*, 185–193.

(81) Cho, S.; Choi, W. Solid-phase photocatalytic degradation of PVC-TiO<sub>2</sub> polymer composites. *J. Photochem. Photobiol., A* **2001**, *143*, 221–228.